

Published in final edited form as:

Proteins. 2004 December 1; 57(4): 850–853. doi:10.1002/prot.10601.

## Crystal Structure of *Bacillus subtilis* YdaF Protein: A Putative Ribosomal *N*-Acetyltransferase

Joseph S. Brunzelle<sup>1</sup>, Ruiying Wu<sup>2</sup>, Sergey V. Korolev<sup>2</sup>, Frank R. Collart<sup>2</sup>, Andrzej Joachimiak<sup>2,\*</sup>, and Wayne F. Anderson<sup>1,\*</sup>

<sup>1</sup>Department of Molecular Pharmacology and Biological Chemistry, Feinberg Medical School, Northwestern University, Chicago, Illinois

<sup>2</sup>Biosciences Division and Structural Biology Center, Argonne National Laboratory, Argonne, Illinois

### Introduction

Comparative sequence analysis suggests that the *ydaF* gene encodes a protein (YdaF) that functions as an *N*-acetyltransferase, more specifically, a ribosomal *N*-acetyltransferase. Sequence analysis using basic local alignment search tool (BLAST) suggests that YdaF belongs to a large family of proteins (199 proteins found in 88 unique species of bacteria, archaea, and eukaryotes). YdaF also belongs to the COG1670,<sup>1</sup> which includes the *Escherichia coli* RimL protein that is known to acetylate ribosomal protein L12. *N*-acetylation (NAT) has been found in all kingdoms.<sup>2</sup> NAT enzymes catalyze the transfer of an acetyl group from acetyl-CoA (AcCoA) to a primary amino group. For example, NATs can acetylate the *N*-terminal  $\alpha$ -amino group, the  $\epsilon$ -amino group of lysine residues, aminoglycoside antibiotics, spermine/speridine, or arylalkylamines such as serotonin.<sup>3</sup>

The crystal structure of the alleged ribosomal NAT protein, YdaF, from *Bacillus subtilis* presented here was determined as a part of the Midwest Center for Structural Genomics. The structure maintains the conserved tertiary structure of other known NATs and a high sequence similarity in the presumed AcCoA binding pocket<sup>3–6</sup> in spite of a very low overall level of sequence identity to other NATs of known structure.

### Experimental

*B. subtilis* acetyltransferase YdaF protein preparation was performed following procedures described previously.<sup>7</sup> The open reading frame of *B. subtilis* YdaF protein was amplified by polymerase chain reaction (PCR) from *E. coli* DH 5 $\alpha$  genomic DNA. The gene was cloned into the pMCSG7<sup>8</sup> using a modified ligation-independent cloning protocol.<sup>9</sup> This process generated an expression clone producing a fusion protein with a *N*-terminal His<sub>6</sub> tag and a Tobacco Etch Virus (TEV) protease recognition site (ENLYFQ↓S). The fusion protein was overproduced in *E. coli* BL21-derivative harboring a plasmid encoding three rare *E. coli* tRNAs [Arg (AGG/AGA) and Ile (ATA)].

The purification procedure used buffers containing 50 mM *N*-2-hydroxyethylpiperazine-*N'*-2-ethanesulfonic acid (HEPES) pH 8.0, 500 mM NaCl, 5% glycerol, and 10, 20, and 250 mM imidazole for the binding, wash, and elution buffers, respectively. The cells were lysed by

© 2004 WILEY-LISS, INC.

\*Correspondence to: Wayne F. Anderson, Department of Molecular Pharmacology and Biological Chemistry, Feinberg Medical School, Northwestern University, 303 East Chicago Ave., Ward Building, Chicago, IL 60611. wf-anderson@northwestern.edu or Andrzej Joachimiak, Biosciences Division and Structural Biology Center, Argonne National Laboratory, Argonne, IL 60439. andrzej@anl.gov..

sonication after adding fresh lysozyme at 1 mg/mL of final concentration in the presence of protease inhibitor cocktails (Sigma). The lysate was clarified by centrifugation and passed through a pre-equilibrated Ni-NTA column (QIAGEN), and the bound protein was removed with elution buffer. The His<sub>6</sub>-tag was removed by cleavage with recombinant His-tagged TEV protease. The cleaved protein was then resolved from the His-tag and His-tagged TEV protease by passing the mixture through a second Ni<sup>2+</sup>-column. The sample buffer was exchanged into 10 mM Tris/HCl pH 7.6, 2 mM dithiothreitol (DTT) using a PD-10 column (Amersham Biosciences) for the crystallization experiments.

The molecular weight of the protein in solution was determined by size exclusion chromatography on a Superdex-200 10/30 column (Amersham Biosciences) calibrated with ribonuclease A (13.7 kDa), chymotrypsinogen A (25 kDa), ovalbumin (43 kDa), and albumin (67 kDa) as standards. The calibration curve of  $K_{av}$  versus log molecular weight was prepared using the equation:  $K_{av} = (V_e - V_o)/(V_t - V_o)$ , where  $V_e$  = elution volume for the protein,  $V_o$  = column void volume, and  $V_t$  = total bed volume.

Diffraction-quality crystals of selenomethionine (SeMet)-derivitized YdaF protein were grown at 22°C using vapor diffusion in hanging drops. The crystallization drops consisted of 2 µL of the protein at 8 mg/mL mixed with 2 µL reservoir solution of 10% polyethylene glycol (PEG) 6K, Na/KPO<sub>4</sub> pH 6.0, NaCl 0.1M. Crystals were flash-frozen in liquid nitrogen with crystallization buffer plus 25% sucrose as cryoprotectant before data collection. The crystals are monoclinic, space group P2<sub>1</sub> (refer to Table I for complete details).

A two-wavelength multiple-wavelength anomalous dispersion (MAD) data set was collected for the peak and edge energies, as determined from a fluorescence scan of a crystal containing SeMet-labeled YdaF protein. The data were processed with HKL2000 and the substructure was determined using the MAD method in SOLVE.<sup>10</sup> This initial step was administered within the Automated Crystallographic System (ACrS).<sup>11</sup> The resulting initial model was 48% complete. The substructure solution was then used to phase the structure within AutoSHARP, utilizing the Bayesian statistical approach in SHARP.<sup>12</sup> The resulting phases and refined substructure were submitted for density modification, phase extension, non-crystallographic symmetry (NCS) averaging, and auto tracing with RESOLVE,<sup>13–15</sup> and the resulting initial model included 68% of the polypeptide chain.

Final refinement was completed with REFMAC<sup>16</sup> using 24 translation, libration, and screw rotation tensor (TLS) groups<sup>17,18</sup> in combination with restrained maximum-likelihood refinement. Manual model building was done using Quanta.<sup>19</sup> Crystal characteristics, data collection, structure solution, and refinement statistics are shown in Table I.

## Results and Discussion

The crystal structure of YdaF protein reveals a hexameric unit with 3<sub>2</sub> symmetry [Fig. 1(a)]. This is consistent with the results of size exclusion chromatography that suggests the protein is a mixture of dimers and hexamers. The observed molecular weight of dimer is 48.8 kDa (expected 42.1 kDa) and molecular weight of hexamer is 128.3 kDa (expected 126.3 kDa). The ratio of dimer to hexamer observed under the conditions of the size exclusion chromatography experiment was 3:2. The crystal structure and solution measurements suggest YdaF is a trimer of dimers.

The monomer unit is a  $\alpha/\beta$  fold characteristic of acetyl transferase domain. The main  $\beta$ -sheet that runs antiparallel ( $\beta$ 2– $\beta$ 5) with  $\alpha$ -helices  $\alpha$ 1 and  $\alpha$ 2 to the left side of the  $\beta$ -sheet,  $\alpha$ -helix  $\alpha$ 3 is cupped within the curved face of the main sheet and helix  $\alpha$ 4 is to the right of helix  $\alpha$ 3, which forms a cleft [Fig. 1(b)]. Structural comparisons were conducted via the DALI server<sup>20</sup> and the top results were for other NATs with probability z scores as high as 12,

although the sequence homology was only 14%. Upon examination of these similar structures, it was determined that the conserved motifs A–D were also present in the YdaF structure. Motifs A and B have been identified as the putative AcCoA binding site in the other NAT structures.<sup>3–6,21,22</sup> Despite the overall low sequence similarity, this region of YdaF appears to exhibit both sequence and structural conservation. Superpositions of the structures found in the DALI search showed low deviation in the core region and higher deviations in the relative positions of helices  $\alpha 1$  and  $\alpha 2$ .

COG1670 is functionally described as an *N*-acetyltransferase and related to the *rimL* gene, which encodes a ribosomal *N*-acetyltransferase that acetylates the ribosomal protein L12 to form L7 on the large ribosomal subunit. YdaF is a member of this COG. The sequence identity between YdaF and RimL is 29%, with 54% of the residues similar. The putative AcCoA binding site of RimL, motifs A and B have 66% and 55% sequence similarity, respectively. It is suspected that YdaF is the *B. subtilis* homologue of RimL.

## Acknowledgments

Atomic coordinates have been deposited in the Protein Data Bank (PDB), with PDB-ID 1NSL. We wish to thank all members of the Structural Biology Center at Argonne National Laboratory for their help in conducting these experiments. This work was supported by the Protein Structure Initiative, NIH grant GM-62414 and JSB was partially supported by American Cancer Society fellowship GMC-98219.

## REFERENCES

1. Tatusov RL, Koonin EV, Lipman DJ. A genomic perspective on protein families. *Science* 1997;278:631–637. [PubMed: 9381173]
2. Polevoda B, Sherman F. N-terminal acetyltransferases and sequence requirements for N-terminal acetylation of eukaryotic proteins. *J Mol Biol* 2003;325:595–622. [PubMed: 12507466]
3. Angus-Hill ML, Dutnall RN, Tafrov ST, Sternglanz R, Ramakrishnan V. Crystal structure of the histone acetyltransferase Hpa2: a tetrameric member of the Gcn5-related *N*-acetyltransferase superfamily. *J Mol Biol* 1999;294:1311–1325. [PubMed: 10600387]
4. Clements A, Rojas JR, Trievel RC, Wang L, Berger SL, Marmorstein R. Crystal structure of the histone acetyltransferase domain of the human PCAF transcriptional regulator bound to coenzyme A. *EMBO J* 1999;18:3521–3532. [PubMed: 10393169]
5. Rojas JR, Trievel RC, Zhou J, Mo Y, Li X, Berger SL, Allis CD, Marmorstein R. Structure of Tetrahymena GCN5 bound to coenzyme A and a histone H3 peptide. *Nature* 1999;401:93–98. [PubMed: 10485713]
6. Trievel RC, Rojas JR, Sterner DE, Venkataramani RN, Wang L, Zhou J, Allis CD, Berger SL, Marmorstein R. Crystal structure and mechanism of histone acetylation of the yeast GCN5 transcriptional coactivator. *Proc Natl Acad Sci USA* 1999;96:8931–8936. [PubMed: 10430873] [comment]
7. Zhang RG, Skarina T, Katz JE, Beasley S, Khachatryan A, Vyas S, Arrowsmith CH, Clarke S, Edwards A, Joachimiak A, Savchenko A. Structure of *Thermotoga maritima* stationary phase survival protein SurE: a novel acid phosphatase. *Structure* 2001;9:1095–1106. [PubMed: 11709173]
8. Stols L, Gu M, Dieckman L, Raffin R, Collart FR, Donnelly MI. A new vector for high-throughput, ligation-independent cloning encoding a tobacco etch virus protease cleavage site. *Protein Express Purif* 2002;25:8–15.
9. Dieckman L, Gu M, Stols L, Donnelly MI, Collart FR. High throughput methods for gene cloning and expression. *Protein Express Purif* 2002;25:1–7.
10. Terwilliger TC, Berendzen J. Automated MAD and MIR structure solution. *Acta Crystallogr D Biol Crystallogr* 1999;55:849–861. [PubMed: 10089316]
11. Brunzelle JS, Shafae JP, Yang X, Weigand S, Renz Z, Anderson WF. Automated crystallographic system for high-throughput protein structure determination. *Acta Crystallogr D Biol Crystallogr* 2003;D59:1138–1144. [PubMed: 12832756]

12. de la Fortelle E, Bricogne G. Maximum-likelihood heavy-atom parameter refinement for multiple isomorphous replacement and multiwavelength anomalous diffraction methods. *Methods Enzymol* 1997;276:472–494.
13. Terwilliger TC. Reciprocal-space solvent flattening. *Acta Crystallogr D Biol Crystallogr* 1999;55:1863–1871.
14. Terwilliger TC, Berendzen J. Discrimination of solvent from protein regions in native Fourier as a means of evaluating heavy-atom solutions in the MIR and MAD methods. *Acta Crystallogr D Biol Crystallogr* 1999;55:501–505. [PubMed: 10089362]
15. Terwilliger TC. Maximum-likelihood density modification. *Acta Crystallogr D Biol Crystallogr* 2000;56:965–972. [PubMed: 10944333]
16. Murshudov GN, Vagin AA, Dodson EJ. Refinement of macromolecular structures by the maximum-likelihood method. *Acta Crystallogr D Biol Crystallogr* 1997;53:240–255. [PubMed: 15299926]
17. Schomaker V, Trueblood KN. On rigid-body motion of molecules in crystals. *Acta Crystallogr B* 1968;24:63–76.
18. Schomaker V, Trueblood KN. Correlation of internal torsional motion with overall molecular motion in crystals. *Acta Crystallogr B* 1998;54:507–514.
19. QUANTA. Molecular Simulations, Inc.; San Diego: 2000.
20. Holm L, Sander C. The FSSP database of structurally aligned protein fold families. *Nucleic Acids Res* 1994;22:3600–3609. [PubMed: 7937067]
21. Hickman AB, Nambodiri MA, Klein DC, Dyda F. The structural basis of ordered substrate binding by serotonin N-acetyltransferase: enzyme complex at 1.8 Å resolution with a bisubstrate analog. *Cell* 1999;97:361–369. [PubMed: 10319816]
22. Peneff C, Mengin-Lecreulx D, Bourne Y. The crystal structures of Apo and complexed *Saccharomyces cerevisiae* GNA1 shed light on the catalytic mechanism of an amino-sugar *N*-acetyltransferase. *J Biol Chem* 2001;276:16328–16334. [PubMed: 11278591]
23. DeLano, WL. The PyMOL molecular graphics system, Version 0.88. DeLano Scientific LLC; San Carlos, CA: 2003.

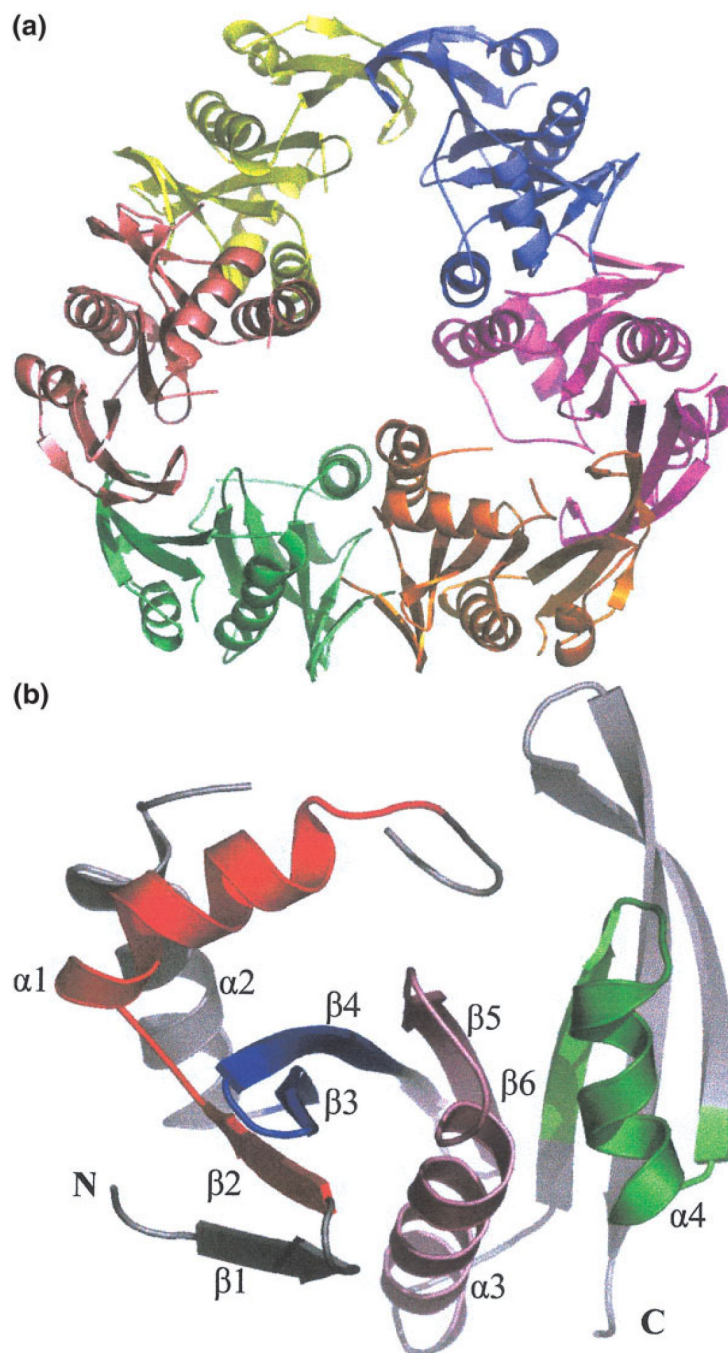


**Fig. 1.** (a) Quaternary structure of YdaF hexamer. View approximately along 3-fold axis, with each of the monomer units represented in a different color. (b) YdaF monomer secondary structure is labeled  $\alpha$  for  $\alpha$ -helix and  $\beta$  for  $\beta$ -sheet from N- to C- terminus. Motifs A–D of acetyl transferase domain are color coded: pink (motif A), green (motif B), red (motif C), and blue (motif D). Figure generated using Pymol.<sup>23</sup>

TABLE I

## Summary of YdaF Crystal Data, MAD Data Collection, and Refinement

Unit cell parameters (angstroms, degrees)	a = 59.339 Å, b = 134.185 Å, c = 91.062 Å, $\alpha = \gamma = 90$ , $\beta = 104.08$	
Space group	P2 <sub>1</sub> (num 4)	
Molecular weight [183 residues (SeMet)]	21,045 Da	
Molecules per asymmetric unit (a.u.)	6	
Selenomethionine residues per a.u.	18	
<b>MAD data</b>	<b>Edge Energy</b>	<b>Peak Energy</b>
Wavelength (Å)	0.9791	0.9792
Resolution limit (Å)	3.1	3.0
Number unique reflections	48,725	53,738
Overall data completeness (%)	100.0	99.4
Overall data redundancy	2.40	3.76
Overall $R_{\text{merge}}$ (%)	10.2	8.6
Figure of merit (FOM)		45.20
Phasing power	1.31	2.65
<b>Resolution range (Å)</b>	<b>20.0–2.7</b>	
Number of reflections (all)	37,877	
Number of reflections (observed)	36,669	
Percent reflections observed	96.8	
$\sigma$ Cutoff	0.0	
Overall $R$ -value (%)	0.2468	
Free $R$ -value (%)	0.2855	
<b>RMS deviations from ideal geometry</b>		
Bond length	0.021	
Angle	2.337	
Dihedral	21.101	
<b>Number of:</b>		
Protein non-hydrogen atoms	8,614	
Water molecules	19	
Chloride ions	6	
Mean B-factor (Å <sup>2</sup> )	30.7	
<b>Ramachandran plot statistics (%)</b>		
Residues in most favored regions	92.5	
Residues in additional allowed regions	7.1	
Residues in generously allowed regions	0.4	
Residues in disallowed region	0.0	